Fusion Engineering and Design Volume 166, May 2021, Article number 112313

Engineering design of a Permeator Against Vacuum mock-up with niobium membrane

F. Papa[a], M. Utili[b], A. Venturini[b], G. Caruso[a], L. Savoldi[c], R. Bonifetto[c], D. Valerio[c], A. Allio[c], A. Collaku[c], M. Tarantino[b]

[a]*DIAEE Department, Sapienza University of Rome, 00186, Rome – Italy*
[b]*ENEA, Department of Fusion and Nuclear Safety Technology, 40032, Camugnano (BO) – Italy*
[c]*Dipartimento Energia "Galileo Ferraris", Politecnico di Torino, Torino (TO) – Italy*

Permeator Against Vacuum (PAV) is one of the technologies proposed for the Tritium Extraction and Removal System (TERS) of the Water-Cooled Lithium Lead Breeding Blanket (WCLL BB). The paper presents the activity aimed at the engineering design of a PAV mock-up with a niobium membrane, in order to later assemble and qualify it. Experience gained in the engineering design of the mock-up, the heating system, the instrumentation, and the vacuum line is illustrated. This experience will be useful for the preliminary design, the manufacturing and the operation of the PAV with niobium membrane for DEMO. Niobium was selected as membrane material of this mock-up because of its high permeability and for its lower cost compared to vanadium, the other candidate material for membranes. Besides, niobium has a lower tendency to oxidation than vanadium. Oxidation would reduce the hydrogen isotopes permeation flux. In this paper, the solution adopted to manufacture the PAV mock-up, a complex component with niobium and P22 parts, is illustrated. The Nb/P22 welding issues are also presented, in particular related to the compatibility of the welded joints with LiPb. In the chosen design, the LiPb flows with two passages in 16 (8+8) niobium "U" shaped pipes installed in a vacuum chamber and welded to a P22 plate. The U-pipes configuration was selected to minimize the welding area, the volume of the component and the membrane thickness while trying to preserve the highest possible extraction efficiency.

Keywords: Tritium extraction, Permeator Against Vacuum, Niobium membrane, Design, Lead lithium.

1. Introduction

The Permeator Against Vacuum (PAV) is one of the selected technologies [1] for the Tritium Extraction and Removal System (TERS) from LiPb in the WCLL BB (Water-Cooled Lithium Lead Breeding Blanket [2]) of DEMO reactor. TERS has two main functions to close the fuel cycle:

- to extract tritium from the flowing LiPb alloy;
- to supply tritium to the Tritium Plant for final processing.

The PAV technology is based on the phenomenon of tritium permeation through a membrane which separates LiPb on one side and vacuum on the other [3]. In this way, a concentration gradient which promotes tritium extraction is established.

In general, tritium transport occurs in two phases: in LiPb and through the membrane.

In the first phase, the tritium dissolved in LiPb spreads into the alloy: tritium migrates in the cloud of Pb atoms, by unbinding from a Li atom and binding to a different Li atom. Along with this diffusion process, an advection contribution has to be considered to describe the tritium behavior, as LiPb is flowing in the PAV.

Tritium transport through the membrane (second phase) occurs in 5 stages [4],[5]: adsorption, absorption, diffusion, recombination and desorption. Starting from the LiPb side, tritium atoms are attracted by the metal membrane (adsorption), which tends to complete its valence orbitals. So, tritium occupies the interstitial sites of the membrane lattice. Then, tritium atoms move from the surface to the bulk of the metal membrane (absorption). Later, tritium diffuses between the interstitial sites due to the concentration gradient (diffusion). When tritium reaches the vacuum-facing side of the membrane, recombination and desorption processes occur, allowing tritium to leave the membrane in a molecular form.

One of the strengths of the PAV is that, once the tritium is extracted from LiPb, there is no need to separate it from a stripping gas, at the contrary of what happens in the Gas-Liquid Contactor extraction technology. This also minimizes the tritium residence time in the system [6].

1. PAV conceptual design

Within EUROfusion project, two configurations and two membrane materials are currently investigated as main alternatives: planar or cylindrical configuration and niobium or vanadium materials.

The planar configuration with vanadium membranes is being investigated in CIEMAT laboratories [7]. In this work, niobium was selected as membrane material for the mock-up because of its high permeability [8] and for its lower cost compared to vanadium (at the time of writing the vanadium price is about 3 times higher than that of niobium). Moreover, this choice was also motivated by the lower tendency to oxidation of niobium with respect to vanadium, as it can be seen in Ellingham diagram (i.e. standard free energy of formation of important oxides as a function of the temperature) [9]. Oxidation would reduce the hydrogen isotopes permeation flux [10]. Regarding the configuration, the cylindrical one was

*Corresponding author: pierdomenico.lorusso@enea.it

chosen in this work to minimize the welding area, the volume/area ratio and the membrane thickness while preserving a high theoretical extraction efficiency.

This configuration minimizes the welding area with respect to the planar configuration because only the ends of the pipes have to be welded, while, using plates, the entire profile as to be welded in order to create a channel. Moreover, using U-pipes and a single collector, it is possible to make a double passage of the LiPb inside the vacuum chamber, making half of the welds.

Using circular pipes instead of rectangular ducts, allows to adopt a lower thickness to withstand the operative loads. A lower thickness enhances the tritium permeation through the membrane.

Therefore, in the selected design, the LiPb flows, in two passage, through 16 niobium "U" shaped pipes installed in a vacuum chamber and welded to an F22 plate (10CrMo9-10, ASTM A182 Grade F22), as shown in Figure 1.

Figure 1: view of PAV mock-up

The actual efficiency of the PAV mock-up will be characterized with TRIEX-II facility, a flowing LiPb facility dedicated to the characterization of TERS technologies, in ENEA Brasimone Research Centre [11]. The conceptual design of this mock-up was made by ENEA and Politecnico di Torino for the WCLL BB [12], while the engineering design was carried out by ENEA and Sapienza University of Rome to adapt the mock-up to the size of TRIEX-II facility. Additional thermal-hydraulic simulations were carried out by Politecnico di Torino, supporting the engineering design.

The efficiency of the PAV is defined as [13]:

$$\eta = 1 - \frac{C_{\mathrm{out,PAV}}}{C_{\mathrm{in,PAV}}} \qquad (1)$$

where, $C_{in,PAV}$ is the hydrogen isotopes concentration at the inlet of the PAV mock-up, while $C_{out,PAV}$ is the hydrogen isotopes concentration at the outlet of the PAV mock-up. In (1), $C_{in,PAV}$ is an input parameter depending on the tritium production rate in the reactor, while $C_{out,PAV}$ depends on the PAV design.

This paper targets the engineering design of the PAV mock-up, with particular attention devoted to the solutions to two challenges of the project, and namely:

- The manufacturing process and in particular the best solution to perform the niobium-F22 joining between the pipes and the plate.
- A heating strategy that does not disturb the tritium diffusion through the niobium membrane, allowing at the same time to keep the temperature at the rated value. The use of conventional heating cables was in fact prevented as they would reduce the permeation area, also adsorbing hydrogen.

2. PAV mock-up description

The geometrical description of the mock-up, the selected instrumentation and the strategy to join F22 and Nb are reported in this section.

2.1 Geometrical description

Geometrically, the PAV mock-up is structured as a tube-and-shell heat exchanger, obtained simplifying the design proposed in [14], see Figure 2.a. The PAV mock-up is composed by a cylindrical vessel with 16 niobium U-tubes, the membranes for hydrogen permeation, welded on a F22 plate. This material has been chosen for his corrosion resistance in LiPb environments. A medium vacuum is pumped in the vessel while the LiPb flows in the niobium pipes. The LiPb is distributed into the niobium pipes by a collector which constitutes the lower part of the PAV. The collector is divided in three parts; each part is connected with one pipe in P22 (10CrMo9-10, ASTM A335 Grade P22), which connects the mock-up with the LiPb loop of the facility. The three pipes are:

- the inlet pipe;
- the discharge pipe;
- the outlet pipe.

The inlet pipe is connected with the part of the collector that allows the LiPb distribution in the first 8 niobium pipes. This part is indicated in red in Figure 2.b. The discharge pipe is connected with the part of the collector (called mixing collector) where the LiPb coming out from the first 8 niobium pipes mixes. From this section of the collector, indicated in yellow in Figure 2.b, the LiPb is distributed in the remaining 8 niobium pipes. The discharge pipe is needed to allow the gravity draining of the mixing collector. The outlet pipe is connected with the section of the collector, indicated in red in Figure 2.b, where the LiPb coming out from the last 8 niobium pipes mixes before leaving the mock-up. Therefore, LiPb will double pass through the vessel, as shown in Figure 2.c and Figure 2.d. The main dimensions of the mock-up are reported in Table 1, while the operative conditions are listed in Table 2. The cylindrical vessel is divided into two

parts so that the upper part can be removed to inspect the Nb pipes or for maintenance. The two parts are joined together by a flange. The upper part is connected to the gas and vacuum line and hosts two feedthrough connectors (in red in Figure 3) for the power supply of the heating systems of niobium pipes (IR lamps, in yellow in Figure 3), which are attached inside the vessel. In this way, when the upper part of the vessel is lifted, the heating systems will also be lifted. Moreover, the upper part of the vessel is equipped with a quartz porthole to allow the visual inspection of the tube bundle also during operation. Quartz has been chosen for its impermeability to hydrogen isotopes [15]. Instead, the lower part of the vessel has two thermocouple feedthrough connectors (in blue in Figure 3), as 50 thermocouples are needed to monitor LiPb temperature in the 16 Nb tubes. The tube plate is wide enough to work also as upper flange of a connection with the collector.

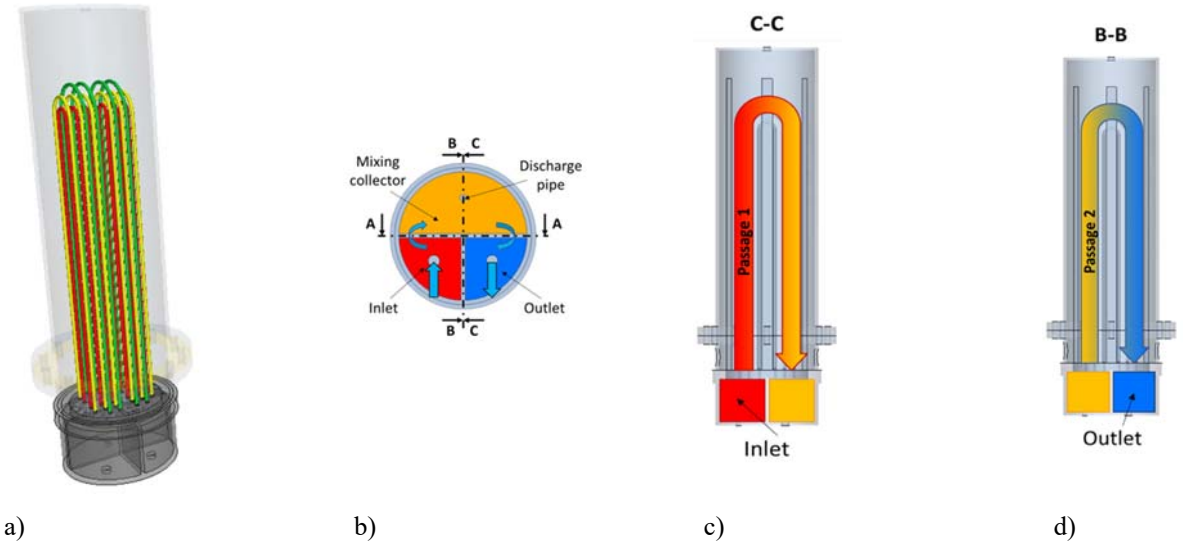

a) b) c) d)

Figure 2: Sketches of the PAV mock-up: (a) simplified sketch of the cylindrical vessel with the 16 niobium U-tubes: Long pipes (L) in green, medium-length pipes (M) in yellow and short pipes (S) in red; (b) horizontal section of the PAV collector showing its 3 parts and the connecting pipes; (c) vertical section of the PAV showing the first passage of LiPb through the vessel; (d) vertical section of the PAV showing the second passage of LiPb through the vessel.

Table 1: main dimensions of the PAV mock-up.

Dimensions	**[mm]**
Height of the vessel	1106.00
External diameter of the vessel	323.85
Thickness of the vessel	6.35
Length of the Nb pipes (including the portions welded in the plate, 30 mm on each side)	1805.25 (S)
	1899.50 (M)
	1993.74 (L)
External diameter of the Nb pipes	10.00
Internal diameter of the Nb pipes	9.20
Pitch of the Nb pipes	30.00
Height of the LiPb collector	156.00
Thickness of the plate	38.00
External diameter of the P22 pipes (inlet/outlet LiPb)	33.40
Thickness of P22 pipes (inlet/outlet LiPb)	3.38
External diameter of the draining pipe	21.34

Thickness of the draining pipe	2.77

Table 2: PAV mock-up operative conditions.

Parameter	Value	Unit
Operative internal pressure of the vessel	10^{-1} - 10^{5}	[Pa]
Max internal pressure of the vessel	$1.1 \cdot 10^{5}$	[Pa]
Max internal pressure of the Nb pipes	$4 \cdot 10^{5}$	[Pa]
Max internal pressure of the LiPb collector	$5 \cdot 10^{5}$	[Pa]
Max temperature of the collector	530	[°C]
Max temperature of the Nb pipes	500	[°C]
Max temperature of the vessel	100	[°C]
Operative LiPb temperature	350-500	[°C]
Max speed of LiPb in the Nb pipes (at 4.6kg/s)	0.97	[m/s]
Total flow rate of LiPb in the Nb pipes	0.2-4.6	[kg/s]
Vessel filling gas (during long stops)	Helium	[-]

Instead, the lower part of the vessel is directly welded on the tube plate, as shown in Figure 4.

Instead, the lower part of the vessel has two thermocouple feedthrough connectors (in blue in Figure 3), as 50 thermocouples are needed to monitor LiPb temperature in the 16 Nb tubes.

The tube plate is wide enough to work also as upper flange of a connection with the collector. Instead, the lower part of the vessel is directly welded on the tube plate, as shown in Figure 4.

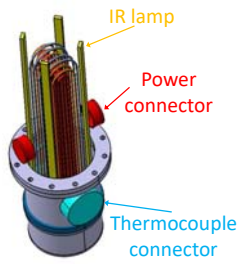

Figure 3: View of PAV connectors and IR lamps

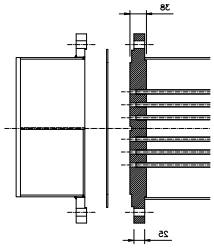

Figure 4: Detail of the connection between F22 plate with the collector

2.2 Joining niobium and F22 steel

The most important issue to be solved in order to manufacture the PAV mock-up was to perform the joining between the niobium pipes and the F22 plate, as there are three main problems to be solved:

- niobium easily oxidizes at high temperatures;
- the melting points of niobium and F22 are very different, so that performing a welding is really difficult;
- most of the brazing alloys are made of materials that are highly soluble in LiPb, such as nickel.

The solution proposed in this paper to join the niobium pipe with the F22 plate is to use a vacuum brazing based on a nickel-based brazing alloy. The vacuum brazing avoids the oxidation of niobium, while, to prevent nickel from solubilizing in LiPb, the brazing procedures are carried out in such a way that avoids the contact between the filler material and the LiPb. The brazing will be performed on almost the entire depth of the plate in order to create a strong joint between the two materials. The brazing alloy can withstand up to 1100°C, about 600°C higher than the operative condition of the mock-up. Each brazing will be later inspected with not destructive testing (radiography).

However, a testing joint has also been assessed with destructive testing before starting the manufacturing, as the brazing of these materials has never been performed earlier. The testing joint will undergo tensile testing to evaluate its resistance.

A thermal analysis of the mock-up, shown in the following section, demonstrated the necessity of additional heating systems to keep constant the temperature of the niobium pipes. For this reason, infrared lamps will be installed in the vessel.

2.3 Heating system of niobium pipes

The heating strategy adopted to keep the LiPb at the rated temperature and to avoid disturbing the tritium diffusion through the niobium membrane is described in this section.

The use of heating cables as heating system would not only be difficult for the installation, since the number of

pipes is high compared to the dimensions of the component, but also the presence of the cables would create an additional obstacle to the diffusion of tritium through the Nb membrane. For these reasons, a different solution is proposed.

The heating system of the niobium pipes will consist of 4 double-tube infrared lamps mounted inside the vessel. The lamps are made of quartz, a material that prevents hydrogen permeation, so that their presence will not affect the measurement of the permeated flux [15]. The lamps will allow to keep the temperature of the Nb pipes at about 450°C to avoid the solidification of the LiPb inside the pipes. The lamps, 100 cm long and positioned symmetrically with respect to the center, will have a maximum power of 3.5 W/cm, they will be 100 cm long and they will have an angle of action of 60°. A lamp and their positions are shown in Figure 5.

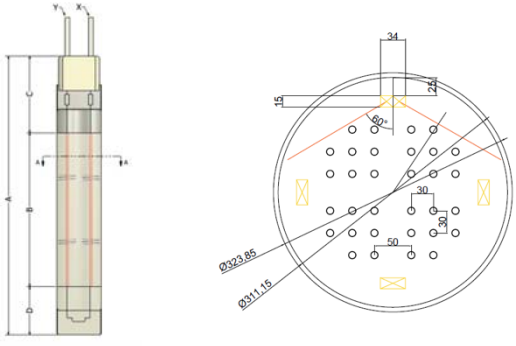

Figure 5: Sketch of an IR lamp and PAV technical drawing, horizontal section of the vessel showing the IR lamps position and their angle of action.

3 Detailed analyses in support of the mock-up design

This section presents the most important calculations that were made in support of the mock-up engineering design. In particular the hydraulic, thermal and mechanical analyses and the tritium transport analysis.

3.1 Hydraulic analysis: flow distribution in the Nb pipes

First, the LiPb flow distribution among the different pipes must be computed to check the homogeneity of the flow distribution: a severe flow unbalance, causing a deviation from the average speed, would affect the extraction efficiency. 3D CFD analyses of the LiPb flow, with special attention to the manifolds (where the flow is split among the pipes), have been carried out using the commercial software STAR-CCM+[16], solving the problem of 3D conjugate heat transfer in the entire mock-up with a segregated solver.

The LiPb flow in the pipes is in turbulent conditions for the entire range of operational mass flow rate. A two-equation Reynolds-averaged Navier–Stokes (RANS) k–ω SST [17] model is adopted in the simulations, with an all-y+ wall treatment. The chosen model SST-Menter k–ω works as a standard k–ω in the near-wall region, and as a k–ε model in the fully turbulent region. The mesh developed to describe the mock-up geometry is reported in Figure 6. While in the manifolds the cell base size is 10 mm for the fluid, a significant refinement (to 1 mm) is needed for the bulk fluid near the inlets and outlets of Nb tubes. Four prismatic layers at the wall allow a good solution of the Navier-Stokes equations in the boundary layer. In the Nb tubes, an extruded mesh with element of 45 mm is used. For the solid computational domain, the mesh is made by a mix of polyhedral cells in thick regions, and prismatic cells, in thin regions, with a base size that locally matches the fluid one. The total number of cells resulted to be 4.5MCells.

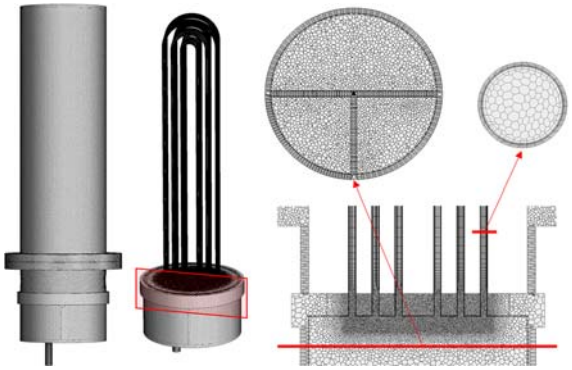

Figure 6: Grid developed for the 3D CFD simulations of the PAV mock-up with its main features: (a) the polyhedral cells in core fluid in the manifold; (b) a finer mesh in the inlet/outlet of the Nb tubes; (c) prism layers at the walls; (d) extruded mesh in the Nb tubes.

Figure 7.a shows that the flow repartition is close to the average value within <5% for different values of the mass flow rates giving an acceptable homogeneity of the speed. Values of maximum speed around 0.5 m/s could be achieved with mass flow rates of 2-2.5 kg/s. Note that the maximum spread between the speed values stays below 0.1 m/s in the worst case (maximum flow rate). The flow repartition shows a slightly lower flow rate in the longest channels, while the shortest channels have on average the largest flow rate, as expected. This is especially true for the second pipe passage, while the first passage is affected by some jet effects from the inlet pipe that affects, in particular, the central pipes, as shown in Figure 8.

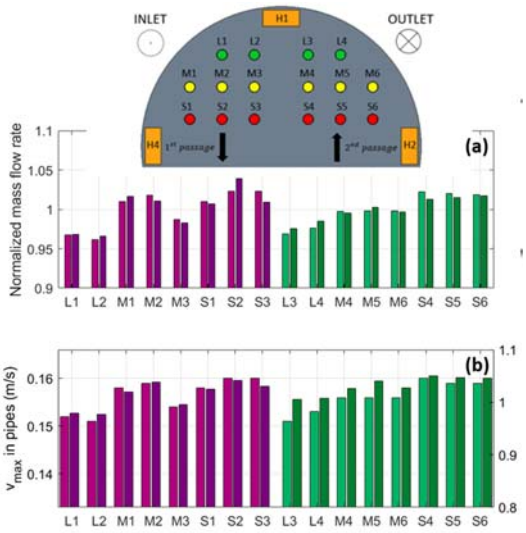

Figure 7: (a) Mass flow rate repartition among the mock-up pipes, normalized to the average value and (b) maximum speed in the pipes (first passage: pipes L1-L2, M1-M3, S1-S3, see inset, and second passage: pipes L3-L4, M4-M6, S4-S6), for the total mass flow rate of 0.75 kg/s (light bars) and 4.5 kg/s (dark bars). In (b), the dark bars refer to the right axis.

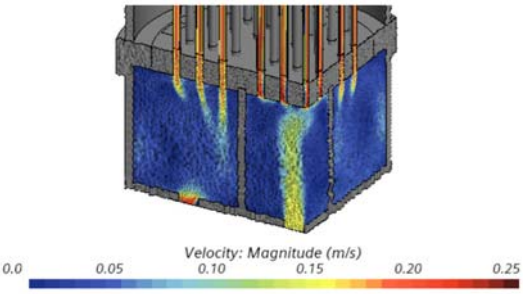

Figure 8: Flow field computed in the manifolds, for a mass flow rate of 0.75 kg/s.

3.2 Thermal analysis: thermal losses from niobium pipes

The steady-state thermal-fluid analysis of the entire mock-up has been performed in the most conservative case (higher LiPb temperature) imposing a uniform temperature of 450°C (723 K) on the outer surface of the manifolds, while allowing convective and radiative heat transfer from the vessel to the environment, assumed at 15°C (288 K), with a heat transfer coefficient of 10 W/m^{2}K [18] and an emissivity of the surface of 0.4 for the vessel wall and of 0.15 for the niobium pipes. The LiPb is entering the manifold conservatively at a constant temperature of 450°C. In the simulations, the internal radiation transfer from the pipes to the vessel is modeled using a surface-to-surface approach, which automatically evaluates the view factors for all the radiative surfaces.

The resulting temperature map in the mock-up is shown in normalized form in Figure 9. While the manifolds are globally at a temperature close to the fluid nominal inlet temperature (as expected, see Figure 9.a), the pipes lose power by radiation to the vessel, which is at the temperature very close to the ambient one. Without an additional heating inside the vessel, at low mass flow rates, the pipes are expected to be at a temperature quite lower than the nominal one, and non-uniform along their length due to the thermal bridge of the plate, see Figure 9.b.

The power balance of the vessel is reported in the Sankey diagram in Figure 10, highlighting the fraction of power in input to the mock-up which is released by the vessel to the environment through convective and radiative heat transfer. At all mass flow rates, the conductive load from the plate roughly balances the convective and radiative losses to the environment. Note that convection dominates over the radiative heat transfer because the small temperature difference between the vessel and the surrounding, see Figure 9.a.

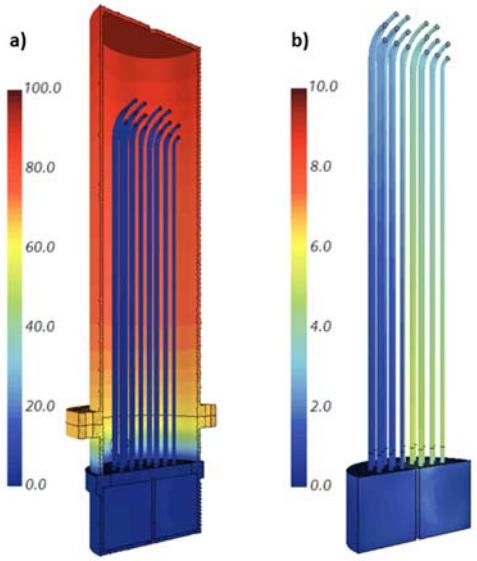

Figure 9: Steady-state normalized temperature difference computed as (Tinlet – T)/(Tinlet – Tambient) in the mock-up (a), with a zoom on the fluid domain (b), for the minimum mass flow rate (0.2 kg/s).

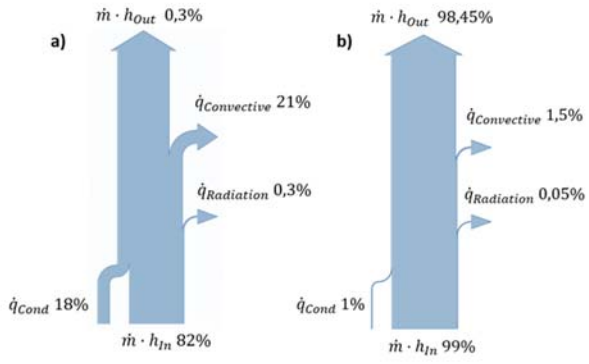

Figure 10: Sankey diagram highlighting the power balance on the mock-up for a mass flow of a) 0.2 kg/s and b) 4.5 kg/s.

3.4 Mechanical analysis and tritium transport analysis

The pre-dimensioning of the mock-up is based on the

actual constraints due to the allowable pressure drop (0.5 bar at the maximum mass flow rate of 4.6 kg/s, given the pump characteristics and the pressure drops of the rest of the loop components) and to the space allocated for its installation in TRIEX-II. The constraints on the dimensions are a maximum manifold height of 160 mm, an allowed height of the niobium pipes of about 1000 mm (including the U curve) and a maximum external diameter of the vessel of 330 mm. The vessel height results about 1160 mm. The minimum pitch among the pipes is 30 mm to allow proper welding in the plate.

The design process is composed of the following steps:

1) The preliminary sizing of the martensitic steel (10CrMo9-10 [19]) vessel and plate thickness using the thick shell theory [20] to withstand the operating (10^{-6} bar) and design (10 bar) pressures in the vessel;

2) The sizing of the niobium pipes (membrane) diameter in order to satisfy the constraints on the pressure drop and maximum dimensions (i.e. assuming the maximum possible membrane length of ~2000 mm), as well as a suitable LiPb speed allowing the best performances in terms of hydrogen permeation [21], computed to be ~0.5 m/s;

3) The design of the layout (and definition of the number) of the niobium pipes to be inserted in the plate, satisfying the given constraint on the pitch.

As a result, the minimum vessel and plate thickness is 4.3 mm and 12 mm, respectively, the Nb pipe inner/outer diameter is 9.2/10 mm [22] and the number of U-pipes per passage is 8.

The mechanical stress was assessed by a thermo-mechanical model, using COMSOL 5.1 Multiphysics tool [23]. The deformation of the upper plate in nominal conditions is presented in Figure **11**. At the junction between the vessel and the plate, the thick shell theory (suitable for cylindrical wall, thick shell and axial symmetry, far from geometrical discontinuities) loses its validity, and indeed the deformation is quite large (although the stress is acceptably below the ~21 MPa limit, accounting for the safety factor from ASME VIII Div.1). This (local) effect can be compensated by a series of clamps, to assure the structural resistance in all operating conditions. Instead, the bottom plate deformation can be seen in Figure 12, conservatively at a LiPb temperature of 500°C and during normal operating conditions.

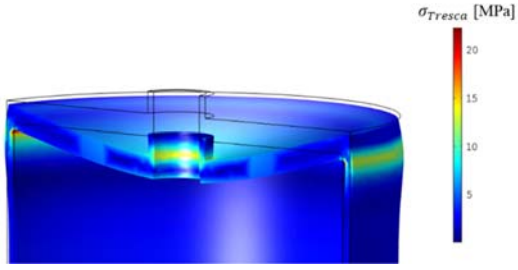

Figure 11: Stress distribution (and deformation) close to the upper plate in normal operating conditions for a PbLi temperature of 330 °C.

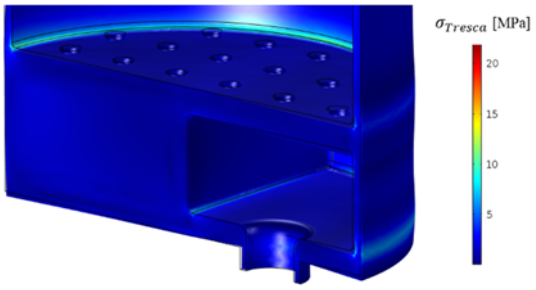

Figure 12. Stress distribution close to the holed plate in normal operating conditions for PbLi temperature of 500 °C.

Finally, the resulting hydrogen extraction efficiency is assessed for the maximum allowed pipe length by means of the surface-limited model (SLM), similar to that described in [21]. The LiPb properties used in the calculations were taken from [24].

Tritium transport can be modelled in two ways: surface-limited regime and diffusion-limited regime. In the diffusion-limited regime [25] the hydrogen isotopes permeation process is limited by the atomic diffusion in the Nb membrane. Instead, the kinetics of Q transport is said to be surface-limited when the surface effects, adsorption and recombination, provide the biggest resistance to permeation [21][26][27][28].

The hydrogen concentration along the LiPb flow direction in the PAV channels is evaluated with a transport model. The pressure gradient between the inner side of the pipes (Nb membrane), where LiPb flows, and the outer side (the vessel) drives the tritium permeation across the pipe wall together with the surface phenomena. The motion of the LiPb, as well as the tritium concentration along the pipe, is modelled by 1D advection equation along the axial coordinate of each pipe

$$\nabla \cdot \vec{J} = -\vec{v} \cdot \nabla C_T$$

where:

- $\vec{J}$ is the tritium mass flux $[\frac{mol}{m^2 \cdot s}]$
- $\vec{v}$ is the speed of LiPb in the pipes $[\frac{m}{s}]$
- C_T is the hydrogen concentration in LiPb $[\frac{mol}{m^3}]$

To correctly identify in which regime the mock-up operates, the dimensionless permeation parameter should be used as a criterion:

$$W = \frac{2K_r t K_s \sqrt{p_{in}}}{D}$$

where:

- K_r is the recombination constant ($[m^4/s/mol]$),
- t is the membrane thickness ([m]),
- K_s is the solubility constant ($[mol/m^3/Pa^{0.5}]$),
- D is the mass diffusion coefficient ($[m^2/s]$) of

the membrane,
- p_{in} is the partial pressure ([Pa]) of the gas impinging on the surface.

This number expresses the ratio among the superficial effects and the diffusion phenomena inside the bulk. Therefore, if W <<1 the regime can be considered surface-limited, whereas a W >>1 implies that the permeation is completely diffusion-driven. An exhaustive explanation on the permeation parameter is reported in [28]. The values used for the evaluation of W are reported in Table 3.

This leads to a $W \sim 4 \cdot 10^{-2}$ for the niobium membrane for T = 330°C.

The permeated flux calculated across the LiPb flow direction is instead evaluated on the basis of the tritium concentration gradient in the pipe cross section, as in the following eq.

$$J_T(r_i, z) = h_T \left(C_{T,b}(z) - C_{T,wall}(z) \right)$$

where

- h_T ($[m/s]$) is the mass transfer coefficient in LiPb, evaluated according to [29]; for a LiPb speed of 0.5 m/s and a temperature of 330°C and 500°C, the h_T is $7 \cdot 10^{-5}$ m/s and $2 \cdot 10^{-4}$ m/s, respectively
- $C_{T,wall}$ is the tritium concentration next to the wall on the LiPb side.

The results of hydrogen extraction efficiency reported in Figure 13 for different LiPb temperatures show that the efficiency is limited by the short length of the mock-up permeator membrane (< 4 m, considering the double passage). The former is representative of a non-oxidized Nb surface, while the latter is the reference for an oxidized membrane surface.

The maximum efficiency of ~50% is reached for high temperature values, while at 330°C the efficiency should be between 5 and 20%.

The physical constants of the Nb membrane and the mass transfer coefficient in LiPb at different temperatures have been evaluated using the references quoted in Table 3 and the correlations in [29], in order to obtain the results shown in Figure 13.

Table 3: Physical constants of the Nb membrane for W at different temperatures at fixed thickness.

T [°C]	K_r [21] $[m^4/s/mol]$	K_s [8] $[mol/m^3/Pa^{0.5}]$	p_{H_2} $[Pa]$	D [8] $[m^2/s]$	t [m]
330	$6.02 \cdot 10^{-11}$	$1.26 \cdot 10^{3}$	100	$6.51 \cdot 10^{-9}$	$0.4 \cdot 10^{-3}$
500	$6.02 \cdot 10^{-7}$	107.64	100	$1.12 \cdot 10^{-8}$	$0.4 \cdot 10^{-3}$

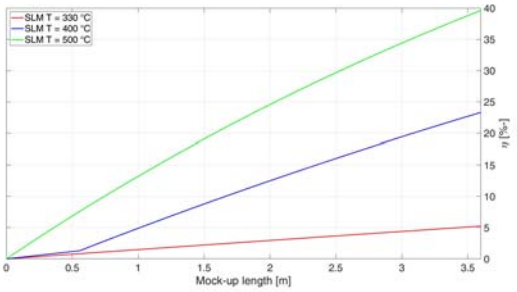

Figure 13: Effect of the variation of the LiPb temperature on the H extraction efficiency
computed by the SLM (flow velocity fixed at 0.5 m/s).

4. Mock-up instrumentation

One of the main aims of the PAV mock-up is to quantify the hydrogen permeation flux through a 0.4 mm thick niobium pipe with flowing LiPb inside and under different working conditions. To this end, a helium leak detector (ASM340 series by Pfeiffer Vacuum) will be connected to the vacuum side of the PAV vessel through a 1/4″ vacuum-tight Swagelok line. The instrument will perform an integral measurement of the permeated hydrogen, from which it will be possible to evaluate the average permeation flux per unit area. This value will be used as a reference for the results of numerical models. The leak detector is equipped with a rotary vane pump with 15 m^3/h backing pump capacity and it has a minimum detectable rate as low as $5 \cdot 10^{-12}$ mbar·l/s.

Heating cables and bands will be used to heat up the collector and the P22 pipes that connect the collector to the facility, to maintain the LiPb that flows in the niobium pipes at 450°C,

In order to control the niobium pipes temperature, 50 thermocouples will be installed at different heights on the pipes. Each pipe will be equipped with two thermocouples at the inlet and outlet. Additionally, six pipes will have one more thermocouple at the top of the U-bend and two more at half height. These six pipes were chosen in order to have a good mapping of the temperature in the various positions, taking advantage of the cylindrical symmetry.

Conclusions

The main objective of this work was to perform the engineering design of a PAV mock-up with niobium membrane with the aim to successively install it in TRIEX-II facility and to characterize its performances.

A cylindrical shape with U-tubes was selected to minimize the overall size of the components, the welding area and the membrane thickness with respect to the planar configuration. Niobium was selected as membrane material for its high hydrogen permeability, its lower tendency to oxidation and its lower cost with respect to vanadium.

The design took into account thresholds for the overall dimensions and pressure losses and was optimized to limit the spread of LiPb speed among the pipes. 0.5 m/s was evaluated the optimal LiPb speed for hydrogen isotopes

permeation. At 500°C, the obtained mock-up shows a theoretical maximum extraction efficiency of about 40%.

Thermal simulations highlighted the need for a heating system to maintain the LiPb temperature almost uniform in the niobium pipes. Quartz-made infrared lamps were chosen as heating system of the Nb pipes for an advantage in installation with respect to heating cables/bands and for the very low permeability of quartz to hydrogen isotopes, thus minimizing the negative influence on the experiments.

A helium leak detector was selected to measure the permeated flux on the vacuum side of the mock-up. The integral measurement of permeated flux will allow to evaluate the permeation per unit area and will be used as reference for the numerical simulations.

The choice of the procedure to join Niobium and F22 ferritic/martensitic steel considered the very different melting points of these materials, the nickel solubility in LiPb and the tendency to oxidation of niobium at high temperature. An innovative vacuum brazing with a nickel-based alloy was developed to overcome these issues. The joint will penetrate almost the entire thickness of the plate and will have high temperature resistance.

Acknowledgments

This work has been carried out within the framework of the EUROfusion Consortium and has received funding from the Euratom research and training programme 2014-2018 and 2019-2020 under grant agreement No 633053. The views and opinions expressed herein do not necessarily reflect those of the European Commission.

References

[1] F. Cismondi et al., Progress of the conceptual design of the European DEMO breeding blanket, tritium extraction and coolant purification systems, Fusion Engineering and Design 157 (2020), 111640.

[2] A. Del Nevo et al., WCLL BB design and Integration studies 2019 activities, February 2020, BB-3.2.1-T006-D001, EFDA_D_2P5NE5.

[3] H. Moriyama et al., Tritium recovery from liquid metals, Fusion Engineering and Design 28 (1995), 226-239.

[4] V. D'Auria et al., Tritium extraction from lithium-lead in the EU DEMO blanket using Permeator Against Vacuum, Fusion Science and Technologies 71 (2017), 537-543.

[5] A. M. Polcaro et al., The Kinetics of Hydrogen Absorption in Molten Pb/Li Alloy, Journal of Nuclear Materials 119 (1983), 291-295.

[6] D. Demange et al., Tritium extraction technologies and DEMO requirements, Fusion Engineering and Design 109–111, Part A (2016), 912-916.

[7] B. Garcinuño et al., Design and fabrication of a Permeator Against Vacuum prototype for small scale testing at Lead-Lithium facility, Fusion Engineering and Design 124 (2017), 871-875.

[8] S. A. Steward, Review of hydrogen isotope permeability through materials, Technical report UCRL-53441, Lawrence Livermore National Laboratory, www.osti.gov/scitech/servlets/purl/5277693, 1983.

[9] L.S. Darken. Physical Chemistry of Metals. ISBN 13: 9780070153554. Mc Graw Hill, 1953.

[10] R.A. Strehlow and H.C. Savage, The Permeation of Hydrogen Isotopes through Structural Metals at Low Pressures and through Metals with Oxide Film Barriers, Nuclear Technology 22 (1974), 127-137.

[11] L. Candido et al., An integrated hydrogen isotopes transport model for the TRIEX-II facility, Fusion Engineering and Design 155 (2020), 111585.

[12] R. Bonifetto et al., Conceptual design of a mock-up for the EU DEMO Tritium Extraction System based on Permeator Against Vacuum technology", presented at the 12th International Conference on Tritium Science and Technology April 22-26, 2019.

[13] M. Utili et al., Investigation on efficiency of gas liquid contactor used as tritium extraction unit for HCLL-TBM Pb-16Li loop, Fusion Engineering and Design 109–111, Part A (2016), 1-6.

[14] V. D'Auria et al., Design of a Permeator-Against-Vacuum mock-up for the tritium extraction from PbLi at low speed, Fusion Engineering and Design 121 (2017) 198-203.

[15] J. E. Shelby, Molecular diffusion and solubility of hydrogen isotopes in vitreous silica, Journal of Applied Physics 48 (1977), 3387-3394.

[16] Star-CCM+ User's Manual, CD ADAPCO, New York, 2019.

[17] F. R. Menter, Two-Equation Eddy-Viscosity Turbulence Models for Engineering Applications, AIAA J. 1994, 32, 1598–1605.

[18] TL Bergman et al., Fundamentals of heat and mass transfer, 2011

[19] Gruppo Lucefin [Online]. Available: www.lucefin.com/wp-content/files_mf/10crmo910.pdf, accessed on 07 Sept. 2020.

[20] S. Timoshenko and J. N. Goodier, Theory of elasticity, McGRAW-HILL, 1951.

[21] M. A. Pick and K. Sonnenberg, "A model for atomic hydrogen-metal interactions-application to recycling, recombination and permeation," J. Nucl. Mater., vol. 131, pp. 208–220, 1985.

[22] Goodfellow: Supplier of materials for research and development [Online]. Available: https://www.goodfellow.com/it/, accessed on 07 Sept. 2020.

[23] COMSOL 5.1 Multiphysics.

[24] D. Martelli, A. Venturini, and M. Utili, "Literature review of lead-lithium thermophysical properties," Fusion Engineering and Design, vol. 138, no. September 2018, pp. 183–195, 2019.

[25] P. W. Humrickhouse and B. J. Merrill, "Vacuum Permeator Analysis for Extraction of Tritium from DCLL Blankets," Fusion Sci. Technol., 68, 295 (2015).

[26] I. Ali-Khan, K. J. Dietz, F. G. Waelbroeck, and P. Wienhold, "The rate of hydrogen release out of clean metallic surfaces," J. Nucl. Mater., vol. 76–77, no. C, pp. 337–343, 1978.

[27] P. L. Andrew and A. A. Haasz, "Models for hydrogen permeation in metals," J. Appl. Phys., vol. 72, no. 7, pp. 2749–2757, 1992.

[28] E. A. Denisov, M. V. Kompaniets, T. N. Kompaniets, and V. I. Spitsyn, "Surface-limited permeation regime in the study of hydrogen interactions with metals," Meas. J. Int. Meas. Confed., vol. 117, no. August 2017, pp. 258–265, 2018.

[29] P. Harriott and R. M. Hamilton, "Solid-liquid mass transfer in turbulent pipe flow," Chem. Eng. Sci., vol. 20, no. 12, pp. 1073–1078, 1965.